SYNTHESIS, STRUCTURAL AND THEORETICAL INVESTIGATION OF SOME NEW SCHIFF BASES AND 1,3,4-OXADIAZOLE COMPOUNDS DERIVED FROM LAURIC ACID

MAHMOOD **H**AMEED **M**AHMOOD* and **M**UHEB **A. S**ADALDIN**
*Dept. of Chemistry, College of Science, University of Duhok, Kurdistan Region-Iraq
**Dept. of Chemistry, College of Science, University of Mosul-Iraq

(Received: February 6, 2023; Accepted for Publication: March 15, 2023)

ABSTRACT

New Schiff bases derivatives from lauric acid were synthesized through the condensation of dodecane methyl ester with hydrazine to give corresponding hydrazide, which react with aromatic aldehyde derivatives to afford dodecanehydrazide-hydrazones derivatives and with carbon disulfide to give 1,3,4-oxadiazole-2-thion. The chemical structures were confirmed by numerous characterization methods; including Infrared, Ultraviolet-Visible, ^{1}H and ^{13}C Nuclear Magnetic Resonance (NMR) measurements. In order to investigate the ^{1}H and ^{13}C Nuclear Magnetic Resonance, vibrational frequencies, Ultraviolet visible spectra, optimized molecular geometry, HOMO & LUMO and other spectroscopic properties, Density Functional Theory (DFT/B3LYP/6-311++G(d,p)) stimulations were carried out.

KEYWORD: Lauric acid, Schiff Bases, Hydrazaide-Hydrazones synthesis, 1,3,4-oxadiazole-2-thion synthesis, DFT, ^{1}H & ^{13}C NMR, UV-Vis, FT-IR.

1-INTRODUCTION

Lauric acid is non-toxic, cheap has a long shelf life like many other fatty acids, and is safe to handle. It finds its primary application in the cosmetics and soap industries. Soaps, made from the reaction of lauric acid and sodium hydroxide. Those substances known as “Schiff Base” (SB) are the products of a carbonyl compound (ketone and aldehyde) that condensed with a primary amine, the C=N which take place C=O group in the presence of an acid or base catalyze (Scheme 1)(Kajal *et al.*, 2013).

Schiff Bases also called imines or azomethine are organic compounds with the general formula R3R2C=NR1 (Qin *et al.*, 2013). Also hydrazide-hydrazone derivatives have played an important role in medicinal chemistry, supramolecular chemistry, and organic chemistry. Additionally, they have been utilized in a variety of applications including therapeutic uses, sensing, molecular switches, and Metallo-assemblies (B. X. Wu *et al.*, 2021).

The functional group of hydrazide-hydrazone SB contains the -CO-NH-N=CH- moiety that has (i) both in solution and in solid form, the double bond of imine (C=N) exhibits photochromism and E/Z isomerism (Su *et al.*, 2013), (ii) the presence of carbonyl (C=O) and imine (C=N) groups, which enhance the coordination capacity of metal ions(Qin and Yang, 2016), (iii) -NH- and/or C=O groups will supply the hydrogen bonds necessary to bind the proper anions/cations and biomolecules (Maniak *et al.*, 2020),

Imines are useful intermediates that can also serve as starting materials for a variety of different reactions during the synthesis process(Nabhan *et al.*, 2022) such as Mannich bases (Abdulghani and Abbas, 2011), indoles (Faraj *et al.*, 2019), beta-lactam (Turan *et al.*, 2016), and numerous reagents, including but not limited to: have been utilized throughout the process of imine synthesis such as lewis acids (Elmacı *et al.*, 2019), metal complex (Orr, Andrews and Blair, 2021), promoted by microwave irradiation(Srivastava, Yadav and Singh, 2021) and ultrasound radiation(Kargar *et al.*, 2021).

In the area of study of coordination chemistry, Schiff base ligands have been the subject of extensive research, primarily due to the ease with which they can be synthesized, their abundance of them, and the electronic properties they possess. Due to its importance in many fields, including metallurgy, organic, photography, metal refining, and analytical chemistry, Schiff base coordination chemistry

has recently gained a lot of attention(January, 2013; Aidi *et al.*, 2018). Because of their diverse bioactivities which include antifungal, antibacterial, insecticidal, herbicidal, anti-cancer, anti-HIV-1, anti-hepatitis, antitumor, and anti-inflammatory properties 1,3,4-oxadiazole and their derivatives have long been considered a central structure in pharmaceutical and pesticide chemistry(Hiremath *et al.*, 2018; Yang, Li and He, 2020).

Herein is describe the synthesis of new Schiff Bases derivatives produced from the condensation reaction of dodecanhydrazide (compound **2**) with aromatic aldehyde derivatives, and synthesis of 1,3,4-oxadiazole-2-thion through the reaction of carbon disulfide and dodecanhydrazide (compound **2**) in the existence of base (KOH) and hydrolysis with acid (Scheme 2). ^{1}H NMR, ^{13}C NMR, UV-Vis, and FT-IR spectroscopy techniques, as well as elemental analysis, were used to experimentally characterize the compound's structure (**2**, **3a-c**, and **5**). By employing the Density Functional Theory (DFT) technique at the level of B3LYP with the 6-311++G(d,p) basis set, we were able to learn about the IR frequencies, optimized molecular geometry, ^{1}H NMR, ^{13}C NMR spectra, and UV-Vis were used to compare the estimated finding of the DFT approach to the experimental data of the molecule (compounds **2**, **3a-c**, and **5**).

2- EXPERIMENTAL

2.1 Material and Methods

All chemical solvents, reagents, and materials were sold from Sigma Aldrich and UNI-CHEM and used without further purification. Analytical thin-layer chromatography (TLC gel 60 F254) was used to track the progression of reactions, and the spot was visualized with ultraviolet (UV) light. Using TMS as an internal standard, (^{1}H & ^{13}C) NMR spectra were captured in DMSO-*d6* and $CDCl_3$ using a Bruker Advance II 400MHz NMR spectrometer. All spectral measurements were carried out using 1-cm quartz cells and a Jenway 6800 U.V-Visible double beam spectrophotometer from the University of Duhok. Using a KBr disk and an FT-IR spectrometer designed and made by Perkin Elmer, all spectral vibration measurements were performed. Electrothermal Mel-temp M206780/02 was used for measuring the melting point. The ChemDraw professional individual ASL SN Win program was used for chemical structure ((http://www.cambridgesoft.com/, 2015).

2.2 Theoretically Details

The complete series of calculations were carried out on a computer with the Gaussian09 program, and GaussView 5.0.9 program(M. J. Frisch, G. W. Trucks, H. B. Schlegel *et al.*, 2015). The theoretical calculations for all compounds were done utilizing the DFT/B3LYP method with the 6-311++G(d,p) basis set. This notation 6-311++G(d,p) basis set hence indicates that each core orbital is described by a single contracted of six GTO primitives, and each valence shell orbital is described by three contractions one with 3 primitives and the other two with one primitive and by adding two asterisks (**) or (d,p) since (d) is used for heavy atoms, while (p) is used for hydrogen atoms, which represents polarization and two plus sign (++) for "+" which represent sp set are used for heavy (non-hydrogen) atoms, while "++" represent s function is used for hydrogen atoms. However, the augmented by diffuse and polarize functions are more accurate(Belaidi, Bouchaour and Maschke, 2014). The gradient-corrected correlational functional of Lee, Yang, and Parr was combined with Becke's exact exchange functional (B3) with three parameters(LYP) (Zhang, Xu and Goddard, 2009; Zhou *et al.*, 2009).

The initial step in these investigations involved using the DFT/B3LYP approach in the Gaussian09 program at the level of 6-311++G (d,p) to determine the geometry of the most conformation for all chemical compounds. The frequencies of the solvent media and gas phase were determined using the optimal geometry and the practical B3LYP approach. The chemical shifts for the compounds ^{1}H and ^{13}C NMR spectra in DMSO and gas phase, (TD-DFT) U.V-Vis and Infrared were calculated with the Gaussian09 program.

2.3 General procedure of synthesis

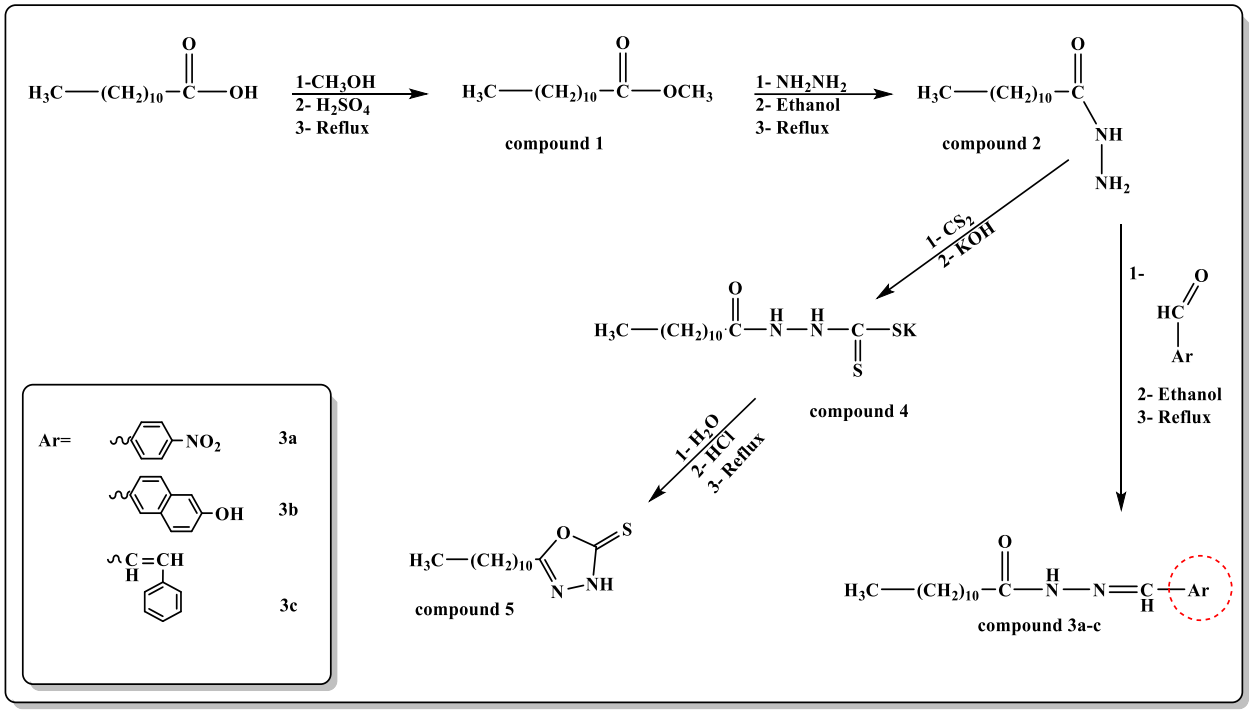

Scheme 1: General chemical reaction for the synthesis of Schiff bases derivatives and 1,3,4-oxadiazol-2-thion.

2.3.1. Synthesis of Methyl Dodecanoate (1)

The esterification of lauric acid with methanol was done in a 50 ml batch reactor equipped with a Dean-Stark apparatus, double-walled air condenser, and magnetic stirrer. A flask with a circular bottom was fitted with a Dean-Stark apparatus so that the water that was produced during the reaction could be separated. The reaction was heated to 110 degree Celsius and allowed to reflux for three hours in the presence of a catalytic amount (1ml) of H_2SO_4 as shown in (Scheme 2) (Brahmkhatri and Patel, 2012). After the reaction was completed, the mixture was cooled to room temperature and then extracted with ethyl acetate separated by a separating funnel we used $MgSO_4$ with cotton to suck the absorb the remaining water in an organic solvent, and the rotatory evaporator was used for separation with ethyl acetate, then the product was saved in an open pharmaceutical glass package about 24h to evaporate residual ethyl acetate to produce 99% yield of light yellow oil, with (260-263^{o}C) boiling point.

2.3.2. Synthesis of Dodecanehydrazide (2)

After dissolving 0.01 mol (2.143 gm) of compound **1** in a 20 ml of absolute ethanol, 0.05 mol (1.602 gm) of hydrazine with a purity of 99% was added to the mixture, drop by drop (Scheme 2). After three hours of being subjected to reflux in a round bottom flask, the mixture was allowed to cool at ambient temperature before being placed in an ice bath to obtain a crystal-white solid product. After that, the product was filtered, washed with cold diethyl ether, and dried (Carpenter, Kenar and Price, 2010). The melting point was between (99-101^{o}C), and the output of the white crystal precipitate was (19.572gm 91%) of the total yield. ^{1}H NMR (400 MHz, DMSO-*d6*), δ; 6.80 (s, 1H), 3.86 (s, 2H), 2.16 (t, *J*=8 Hz, 2H), 1.69-1.61 (m, 2H), 1.33-1.27 (m, 16H), 0.90 (t, *J*= 8 Hz, 3H). ^{13}C NMR (100 MHz, DMSO-*d6*), δ; 174.1, 34.6, 31.9, 29.6, 29.5, 29.5, 29.3, 29.3, 29.3, 25.5, 22.7, 14.1. FT-IR cm^{-1}; 3317, 3290, 3178, 3043, 2954, 2920, 2846, 1627, 1535, 1377, 1010, 690, 617.

2.3.3. General procedure for the synthesis of Schiff Base compounds (3a-c)

Condensation of 0.0015 moles (0.3215 gm) of dodecanhydrazide with 0.0015 moles of aromatic aldehyde derivatives took place in ethanol while the mixture was agitated and refluxed. After the chemical reaction was finished, the mixture was allowed to return to room temperature before being poured into cold water. After that, the result was filtered and then dried. Recrystallization in ethanol was used to purify all of the products, and their purity was checked using thin-layer chromatography (TLC) with a mobile phase that consists of a mixture of hexane and ethyl acetate (19:3) by volume. The melting point was then determined (Scheme 2).

2.3.3.1. N'-(4-nitrobenzyleden) dodecanehydrazide (3a)

Compound **2** was mixed with an equal amount (0.0015 mol, 0.2266 gm) of *p*-nitrobenzaldehyde in 15 ml of ethanol; left the mixture for 3 hours under reflux, after the refluxing process is over, put a mixture away from the heat to cool and settle. We notice that precipitate forms over time. However, it was added to the beaker that contains cold distilled water. The round was washed more than once while moving the beaker on the stirrer and putting a little salt to settle down the precipitate and then the Buchner funnel was used for filtration. The precipitate was purified by recrystallization with hot ethanol to give an 82% yield of crystal light yellow precipitate with a melting point (127-132 ºC). ^{1}H NMR (400 MHz, DMSO-*d6*), δ; 11.64 (s, 1H), 8.28-8.23 (m, 2H), 8.05 (s, 1H), 7.94-7.87 (m, 2H), 2.22 (t, *J*=8 Hz, 2H), 1.61-1.53(m, 2H), 1.29-1.19 (m, 16H), 0.83 (t, *J*=8 Hz, 3H); ^{13}C NMR (100 MHz, DMSO-*d6*), δ; 175.2, 169.6, 148.1, 143.7, 141.1, 140.4, 128.3, 127.9, 34.7, 32.2, 29.5, 29.4, 29.3, 29.2, 29.2, 29.1, 25.4, 24.7, 14.4; FT-IR cm^{-1}, 3086, 2924, 2852, 1666, 1581, 1521, 1394, 1342, 1107, 937, 850, 567, 451.

2.3.3.2. N'-((6-hydroxynaphthalen-2-yl) methylene) dodecanehydrazide (3b)

Compound **2** and 0.2582 gm of 6-hydroxy-2-naphthaldehyde were mixed in 15 ml of ethanol. The mixture cooled and settled after 3 hours of refluxing. As time passes, precipitation forms. But it went into ice-cold water. The round was washed many times while the beaker was stirred, salt was added to aid precipitate settling, and the Buchner funnel was used for filtration. The product was washed, dried, and recrystallized with ethanol to obtain 73% yield crystal light white precipitate with a melting point range of (135-138^{0}C). ^{1}H NMR (400 MHz, D-DMSO), δ; 11.34 (s, 1H), 9.97 (s, 1H), 8.26 (s, 1H), 8.09 (s, 1H), 7.94-7.90 (m, 1H), 7.83-7.77 (m, 2H), 7.70-7.69 (d, *J*=4 Hz, 1H), 7.15-7.13 (m, 1H), 2.21 (t, *J*=8Hz, 2H), 1.64-1.56 (m, 2H), 1.28-1.17 (m, 16H), 0.81 (t, *J*=8 Hz, 2H); ^{13}C NMR (100 MHz, D-DMSO), δ; 174.7, 169.1, 156.9, 143.4, 135.8, 130.3, 129.5, 128.8, 127.8, 127.1, 119.5, 109.5, 34.7, 32.3, 29.6, 29.5, 29.5, 29.3, 29.3, 29.2, 25.6, 24.8, 14.4; FT-IR CM^{-1}, 2334, 2920, 2850, 1664, 1548, 1388, 1182, 875, 665, 478.

2.3.3.3. N'-(3-phenylallylidene) dodecanehydrazide (3c)

An equal volume of starting material compound **2** and (0.1982 gm) of cinnamaldehyde were mixed in 15 ml of absolute ethanol. The mixture was taken from the heat to cool and stable after 3 hours of refluxing. As we can see, a precipitate develops over time. However, it was added to the beaker of icy water. A little salt was added to aid in the precipitate's settlement, several washes of the round were performed while the beaker was being stirred, and then filtration with a Buchner funnel was performed. The products were washed, dried, and improved to provide a 70% yield of white crystal precipitate by recrystallizing it in hot ethanol, Melting point range of (104-110ºC). ^{1}H NMR (400 MHz, D-DMSO), δ; 11.23 (s, 1H), 7.94-7.92 (d, *J*=8 Hz, 1H), 7.80-7.78 (d, *J*=8 Hz, 1H), 7.60-7.57 (m, 2H), 7.40-7.35 (m, 2H), 7.33-7.29 (m, 1H), 6.99-6.92 (m, 1H), 2.16 (t, *J*=8 Hz, 2H), 1.56-1.48 (m, 2H),1.28-1.18 (m, 2H), 0.84 (t, *J*=8 Hz, 3H); ^{13}C NMR (400 MHz, D-DMSO), δ; 174.6, 169.0, 148.1, 145.5, 138.9, 138.5, 136.4, 127.4, 125.8, 34.6, 32.1, 29.5, 29.4, 29.3, 29.2, 29.2, 29.1, 25.4, 24.6, 14.4; FT-IR cm^{-1}, 3199, 3049, 2920, 2852, 1666, 1544, 1382, 1219, 1114, 970, 750, 696, 509.

2.3.3.4. Synthesis of potassium-2-dodecanylhydrazine-1-carbodithioate (4)

(0.005 mole, 1.0717 gm) of compound **2** was dissolved in 10 ml of absolute ethanol and added (0.005 mole, 0.2805 gm) of potassium hydroxide (KOH), and (0.007 mole, 0.5329gm) of carbon disulfide (CS_2), the reaction remained at room temperature with continuous stirring for two hours to obtain a white precipitate salt. We washed with ether, dried it, and weighed it to get 71% of yield, and its melting (148ºC).

2.3.3.5 5-undecyl-1, 3, 4-oxadiazole-2(3H)-thione (5)

In the first step, we dissolved (0.0005 mol, 0.1649 gm) of compound **4** in hot distilled water and then added the HCl (10%) until the solution is converted from basic to acidic and after that left the solution for 2 hours for refluxing. After refluxing put the solution away from the heat to cool off at room temperature then in an ice bath we noticed the white precipitate formed. After filtration, we wash with water more than three times to remove residual HCl, dried, and weighed them to get 74% yield. ^{1}H NMR (400 MHz, $CDCl_3$), δ; 11.16 (s, 1H), 2.69 (t, *J*=8 Hz, 2H), 1.78-1.70 (m, 2H), 1.32-1.25 (m, 16H), 0.88 (t, *J*=8 Hz, 3H). ^{13}C NMR (100 MHz, $CDCl_3$), δ; 178.6, 164.8, 31.9, 29.6, 29.4, 29.3, 29.2, 29.0, 28.8, 25.7, 25.6, 22.7, 14.1. FT-IR

cm^{-1}; 3444, 2920, 2850, 1654, 1554, 1415, 1068, 1026, 948, 717, 605.

3. RESULT AND DISCUSSION

3.1 Synthesis

The preparations of hydrazide-hydrazones Schiff bases (compound **3a-c**) have occurred via four steps as shown in (Scheme 2). Initially, methyl lautare (compound **1**) was prepared from lauric acid esterified with methanol by reflux, and then the prepared product was reacted with hydrazine to produce hydrazide (compound **2**). After that, the dodecanhydrazide (compound **2**) was reacted with different aromatic aldehyde derivatives in the equimolar ratio in ethanol refluxed for 3-6 hours followed by the elimination of one water molecule in the formation of hydrazide-hydrazone SB (compounds **3a-c**), and 1,3,4-oxadiazole-2-thion was prepared by the reacting of compound **2** with carbon disulfide in the presence of a base and hydrolysis with acid, the yields and Melting points shown in Table 1. UV-Vis, FT-IR, and ^{1}H-^{13}C NMR spectroscopy were all used to confirm the chemical structure of each compound. The DFT calculations also looked into the spectroscopic (IR, ^{1}H-^{13}C NMR, and UV-Vis), electronic molecular, and geometric (structural) behaviors of all compounds.

Table (1): The formula, yield, and physical properties for compounds (**1, 2**, **3a-c**, **4,** and **5**).

Compounds	Chemical formula	% yield	M.p. and B.p.	Color of precipitate
1	$C_{13}H_{26}O_2$	99%	260-264°C	Light yellow oil
2	$C_{12}H_{26}N_2O$	91%	99-101°C	Crystal white
3a	$C_{19}H_{29}N_3O_3$	82%	127-132°C	Crystal light yellow
3b	$C_{23}H_{32}N_2O_2$	73%	135-138°C	Crystal light white
3c	$C_{21}H_{32}N_2O$	70%	104-110°C	Crystal white
4	$C_{13}H_{25}N_2OS_2K$	71%	148°C	White
5	$C_{13}H_{24}N_2OS$	74%	69-75°C	White

3.2 ^{1}H and ^{13}C NMR Analysis

The structure of an organic substance can be learned with the help of nuclear magnetic resonance spectroscopy (NMR). Predictions of NMR spectra and investigations into the correlation between chemical shifts and molecular structure are both areas where quantum chemical calculations have proven to be reliable (Gökce *et al.*, 2017; Singh *et al.*, 2017). Accordingly, it is essential to combine theoretical and experimental approaches for understanding and predicting molecular structure(Rosaleen J. Anderson, 2010).

In the present work, ^{1}H & ^{13}C NMR spectra of compounds **2**, and **3a-c** were recorded experimentally in DMSO-d6 and compound **5** in $CDCl_3$. The ^{1}H and ^{13}C NMR spectra were calculated using the optimized geometry of all compounds and the B3LYP method with 6-311++G(d,p) basis set in the Gaussian09 program using the standard gauge-including atomic orbital (GIAO). The chemical shifts of the ^{13}C and ^{1}H NMR spectra of all compounds, both actual and theoretical, are shown in Table 2a-e.

Table (2a): Geometry optimized structure, experimental, and theoretical chemical shift ^{1}H & ^{13}C NMR for compound **2**.

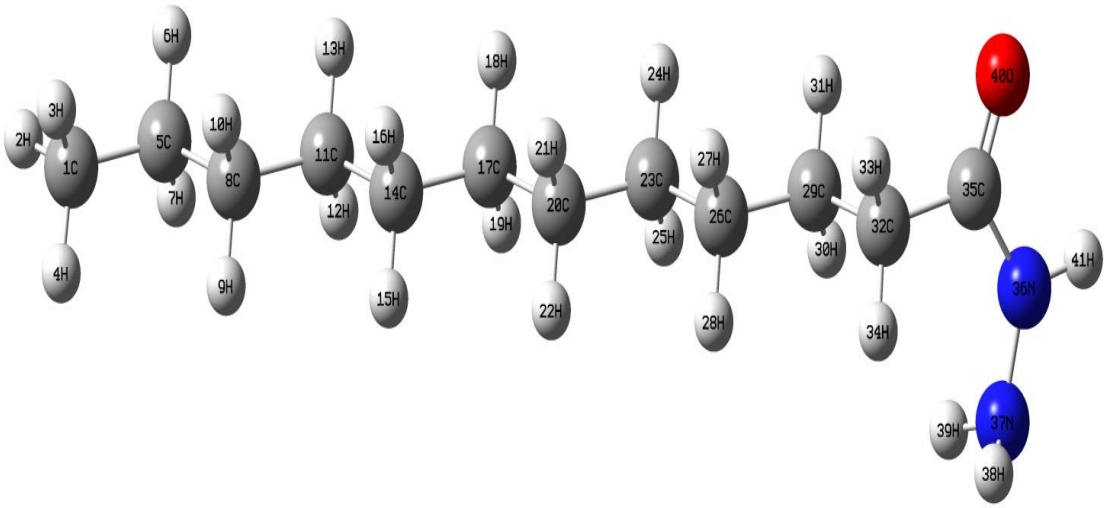

^{1}H NMR			**^{13}C NMR**		
Atoms	**$\delta_{exp.}$(in DMSO-d_6)**	**$\delta_{theo.}$(in DMSO)**	**Atoms**	**$\delta_{exp.}$(in DMSO-d_6)**	**$\delta_{theo.}$(in DMSO)**
$H_{(2,3,4)}$	0.90 (t, *J*=8 Hz, 3H)	1.10, 0.83, 0.83	C1	14.1	14.2
			C5	22.7	27.5
$H_{(6\text{-}28)}$	1.33-1.27 (m, 16H)	1.31-1.19	C8	34.6	37.1
			C11	29.3	35.5
$H_{(30,\ 31)}$	1.69-1.61 (m, 2H)	1.51, 1.39	C14	29.5	35.5
			C17	29.5	35.5
$H_{(33,34)}$	2.16 (t, *J*= 8 Hz, 2H)	2.85, 1.72	C20	29.3	35.4
			C23	29.3	35.2
H_{41}	6.80 (s, 1H)	5.97	C26	29.6	35.7
			C29	25.5	31.7
$H_{(38,39)}$	3.86 (s, 2H)	3.85, 3.84	C32	31.9	35.8
			C35	174.1	184.5

Table (2b): Geometry optimized structure, experimental, and theoretical chemical shift of ^{1}H & ^{13}C NMR for compound **3a**.

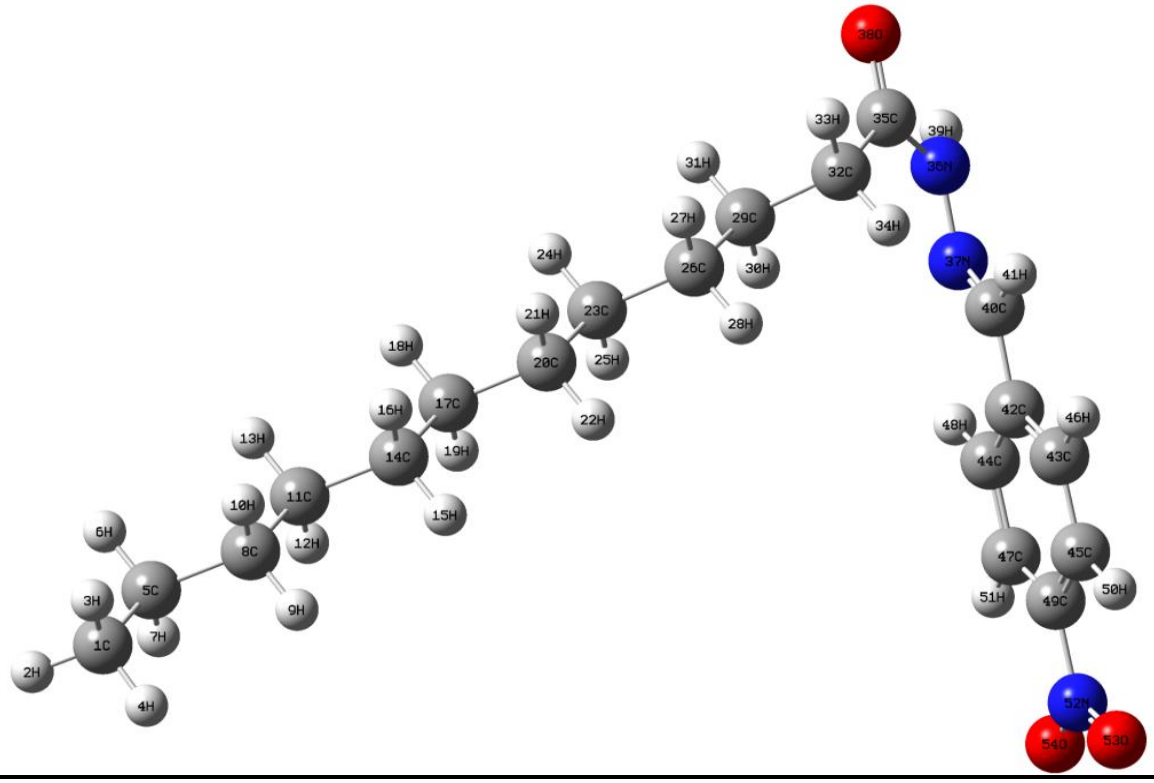

^{1}H NMR			**^{13}C NMR**		
Atoms	**$\delta_{exp.}$(in DMSO-d_6)**	**$\delta_{theo.}$(in DMSO)**	**Atoms**	**$\delta_{exp.}$(in DMSO-d_6)**	**$\delta_{theo.}$(in DMSO)**
$H_{(2,3,4)}$	0.83 (t, *J*=8 Hz, 3H)	0.32, 0.02, 0.02	C1	14.4	10.9
			C5	24.7	25.1
$H_{(6-28)}$	1.29-1.19 (m, 16H)	0.48-0.19	C8	32.2	35.7
			C11	29.1	34.1
$H_{(30,31)}$	1.61-1.53(m, 2H)	0.92, 0.34	C14	29.2	34.2
			C17	29.2	33.9
$H_{(33,34)}$	2.22 (t, *J*=8 Hz, 2H)	2.26, 1.64	C20	29.3	33.9
			C23	29.4	33.1
H_{39}	11.64 (s, 1H)	7.71	C26	29.5	33.3
			C29	25.4	25.6
H_{41}	8.05 (s, 1H)	8.84	C32	34.7	39.6
			C35	175.2	209.2
$H_{(46m51)}$	7.94-7.87 (m, 2H)	8.16,8.53	C40	169.6	180.2
			C42	143.7	158.0
$H_{(48,50)}$	8.28-8.23 (m, 2H)	8.60, 8.70	C44	141.1	142.2
			C47	140.4	141.3
			C49	148.1	163.3
			C45	128.3	138.9
			C43	127.9	139.2

Table (2c): Geometry optimized structure, experimental, and theoretical chemical shift of ^{1}H &^{13}C NMR for compound **3b**.

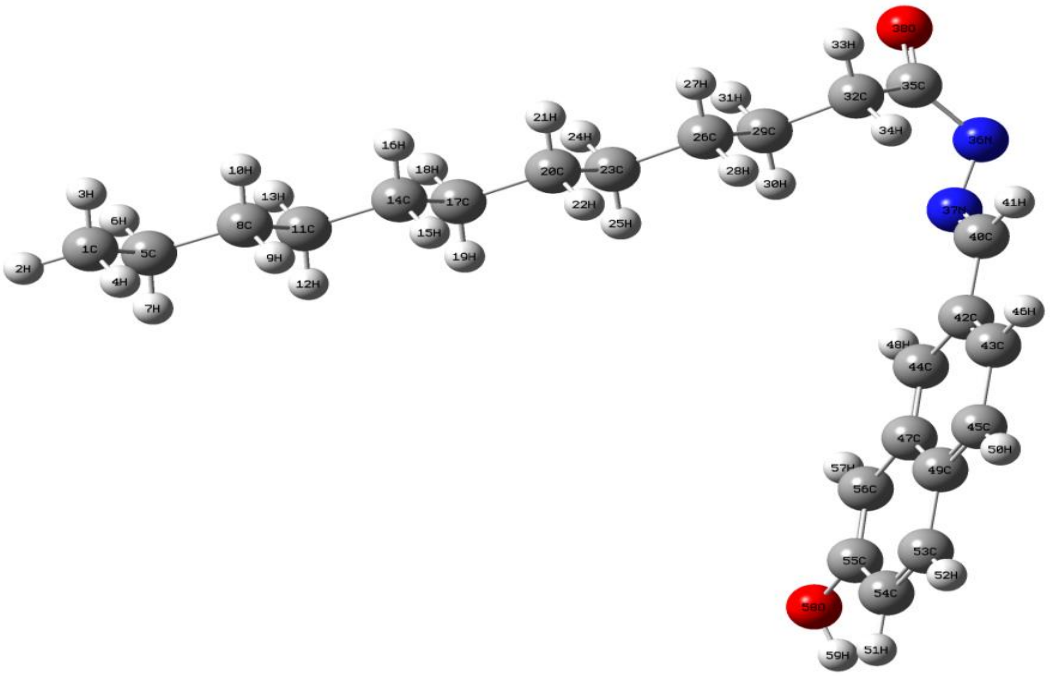

^{1}H NMR			^{13}C NMR		
Atoms	**$\delta_{exp.}$(in DMSO-d_6)**	**$\delta_{theo.}$(in DMSO)**	**Atoms**	**$\delta_{exp.}$(in DMSO-d_6)**	**$\delta_{theo.}$(in DMSO)**
$H_{(2,3,4)}$	0.81 (t, *J*=8 Hz, 2H)	1.07, 0.74, 0.73	C1	14.4	15.1
			C5	24.8	27.7
$H_{(6\text{-}28)}$	1.28-1.17 (m, 16H)	1.19-0.83	C8	34.7	37.3
			C11	29.5	36.0
$H_{(30,31)}$	1.64-1.56 (m, 2H)	1.45, 1.12	C14	29.5	35.8
			C17	32.3	36.4
$H_{(33,34)}$	2.21 (t, *J*=8 Hz, 2H)	2.74, 1.83	C20	29.3	35.7
			C23	29.3	35.8
H_{39}	11.34 (s, 1H)	7.35	C26	29.2	35.3
			C29	25.6	28.5
H_{41}	8.09 (s, 1H)	8.61	C32	29.6	36.2
			C35	174.7	181.6
H_{48}	8.26 (s, 1H)	9.10	C40	169.1	171.5
			C42	129.5	132.8
$H_{(50,56)}$	7.94-7.78 (m, 2H)	8.24, 8.05	C44	130.3	134.0
			C47	127.8	130.8
H_{46}	7.69 (t, *J*=8 Hz, 1H)	7.69	C49	143.4	142.3
			C45	128.8	132.7
$H_{(51,57)}$	7.15-7.10 (m, 2H)	7.49, 7.37	C43	127.1	130.3
			C55	109.5	112.3
H_{59}	9.97 (s, 1H)	5.06	C54	156.9	162.8
			C53	119.5	122.3
			C52	135.8	137.4

Table (2d): Geometry optimized structure, experimental, and theoretical chemical shift of ^{1}H & ^{13}C NMR for compound **3c**.

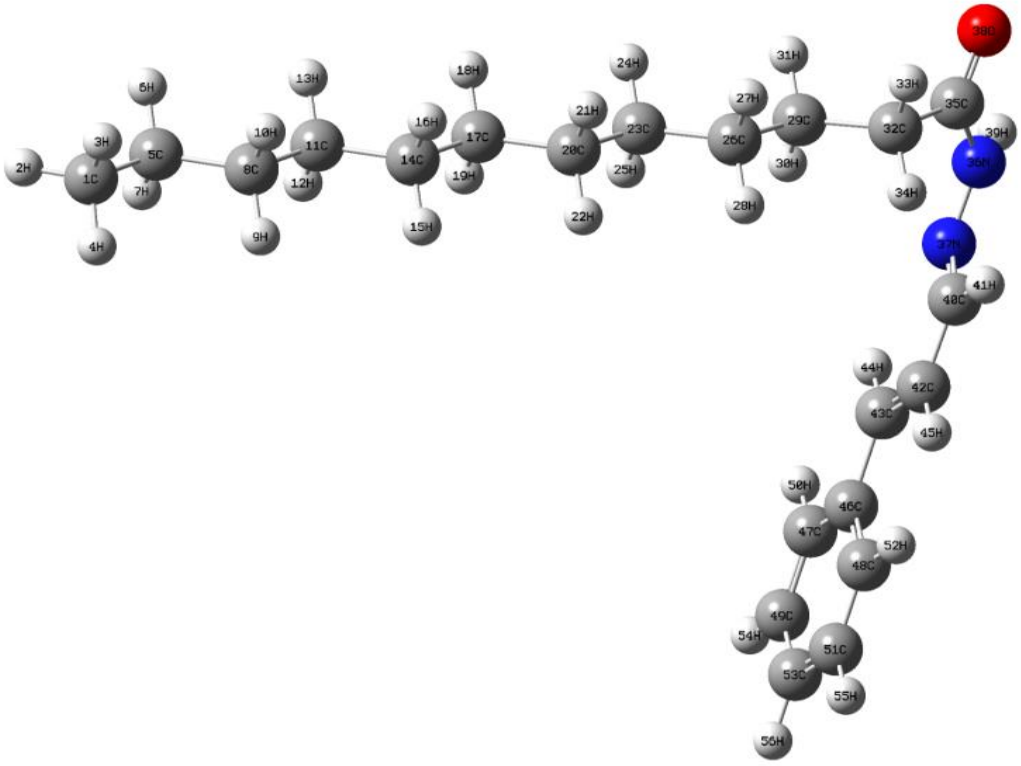

^{1}H NMR			**^{13}C NMR**		
Atoms	**$\delta_{exp.}$(in DMSO-d_6)**	**$\delta_{theo.}$(in DMSO)**	**Atoms**	**$\delta_{exp.}$(in DMSO-d_6)**	**$\delta_{theo.}$(in DMSO)**
$H_{(2,3,4)}$	0.84 (t, *J*=8 Hz, 3H)	1.25, 0.83, 0.80	C1	14.4	14.6
			C5	24.6	27.1
$H_{(6\text{-}28)}$	1.28-1.19 (m, 2H)	1.29- 1.01	C8	34.6	36.7
			C11	29.4	35.5
$H_{(30,31)}$	1.56-1.48 (m, 2H)	1.44, 1.15	C14	29.1	34.4
			C17	32.1	35.7
$H_{(33,34)}$	2.16 (t, *J*=8 Hz, 2H)	2.80, 1.86	C20	29.1	34.2
			C23	29.3	35.3
H_{39}	11.23 (s, 1H)	7.58	C26	29.2	34.9
			C29	25.4	28.9
H_{41}	7.94-7.92 (d, *J*=8 Hz, 1H)	8.37	C32	29.5	35.5
			C35	174.6	180.0
H_{45}	6.99-6.92 (m, 1H)	7.26	C40	169.0	167.9
			C42	125.8	123.7
H_{44}	7.80-7.78 (d, *J*=8 Hz, 1H)	8.36	C43	148.1	143.4
			C46	145.5	141.0
$H_{(50,52)}$	7.60-7.57 (m, 2H)	8.34, 7.89	C47	138.9	138.2
			C49	136.4	134.3
$H_{(54,55)}$	7.40-7.35 (m, 2H)	7.78, 7.92	C53	138.5	135.7
			C51	136.1	134.0
H_{56}	7.33-7.29 (m, 1H)	7.79	C48	127.2	129.8

Table (2e): Geometry optimized structure, experimental, and theoretical chemical shift of ^{1}H & ^{13}C NMR for compound **5**.

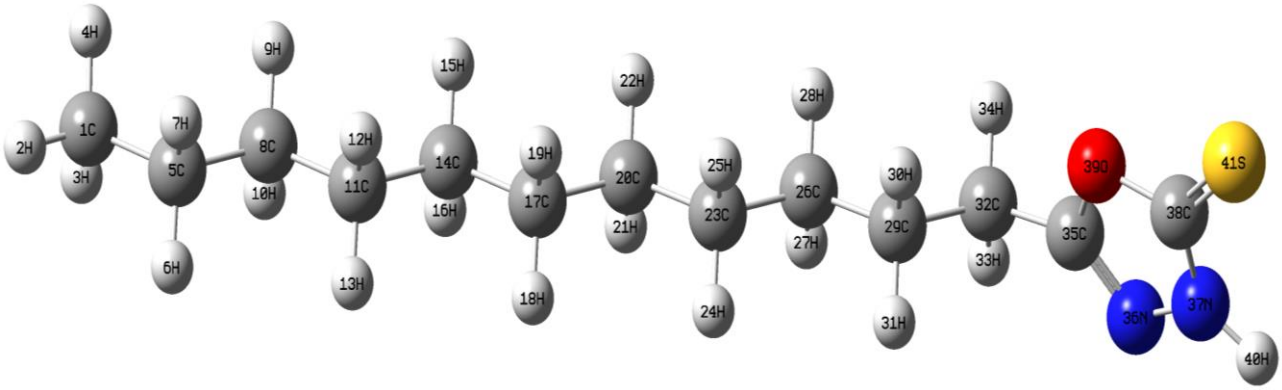

^{1}H NMR			^{13}C NMR		
Atoms	**$\delta_{exp.}$(in DMSO-d_6)**	**$\delta_{theo.}$(in DMSO)**	**Atoms**	**$\delta_{exp.}$(in DMSO-d_6)**	**$\delta_{theo.}$(in DMSO)**
$H_{(2,3,4)}$	0.88 (t, *J*=8 Hz, 3H)	0.36, 0.02, 0.013	C1	14.1	10.9
			C2	22.7	25.4
$H_{(6\text{-}28)}$	1.32-1.25 (m, 16H)	0.61-0.45	C3	31.9	35.5
			C4	29.3	34.7
$H_{(30,31)}$	1.78-1.70 (m, 2H)	0.96, 0.64	C5	29.2	34.3
			C6	29.3	34.5
$H_{(33,34)}$	2.69 (t, *J*=8 Hz, 2H)	2.37, 2.09	C7	29.0	33.9
			C8	28.8	33.7
H_{40}	11.16 (s, 1H)	6.00	C9	25.7	33.5
			C10	25.6	32.4
			C11	29.6	34.8
			C12	164.8	188.3
			C14	178.6	215.4

The chemical shift of ^{1}H NMR values was experimentally determined between δ 0.58-13.27 ppm in DMSO-*d6* and $CDCl_3$, even though theoretically chemical shifts were only noticed to occur in the δ 0.02-9.76 ppm in DMSO. In the experimental ^{1}H NMR spectrum of compound **2**, the sharp to broad singlet signal at δ 6.80 ppm was indicated to –NH proton, while δ 11.23-11.64 ppm was assigned to –NH proton of the hydrazide-hydrazone SB (compounds **3a-c**) and 1,3,4-oxadiazole-2-thion (compound **5**). Hydrazide-hydrazone Schiff base proton (-NH) and 1,3,4-oxadiazole-2-thion proton (-NH) are usually observed at δ 10-12 ppm because of the deshielded effect, and they can be appeared as sharp to broad singlet's due to the chemical exchange (Raczuk *et al.*, 2022). The 1H NMR spectra of the azomethine group (HC=N) for compounds (**3a-c**) were indicated as a singlet at range δ 7.92-8.09 ppm (in DMSO) experimentally and computed δ 8.37-8.84 ppm (in DMSO) for the B3LYP method with the 6-311++G(d,p) basis set. The broad singlet signal at δ 9.97 ppm was assigned to the –OH proton of the alcoholic group in compound **3b**. The theoretical proton resonance signal of –OH was obtained at δ 5.07 ppm (in DMSO) with B3LYP method 6-311++G(d,p) basis set. The ^{1}H NMR chemical shift value of the $–NH_2$ protons appeared at δ 3.85-3.84 ppm (in DMSO) theoretically, while experimentally appear as a broad singlet at δ 3.86 ppm (in DMSO). The signal for the aromatic protons of the compounds **3a-c** was attained as a set of singlet, doublet, and multiplied in the range δ 7.10-8.28 ppm (in

DMSO) and theoretically observed between δ 7.37 and 9.10 ppm (in DMSO).

The ^{13}C NMR resonance signals of the compounds (**2**, **3a-c**, and **5**) appeared in the region of δ 14.1-175.2 ppm in DMSO-d_6 and $CDCl_3$ experimentally, while they were calculated at the range of δ 10.9 and 209.2 ppm (in DMSO) as theoretically. The ^{13}C NMR chemical shifts value of the C1, C5, C8, C11, C14, C17, C20, C23, C26, C29, and C32 atoms, which are aliphatic and were found to be lower than those of the other carbons that are close to the electronegative atom C12 and C16 in all compounds. The carbon resonance signals of aliphatic carbons were recorded experimentally in DMSO-d_6 at δ 14.1-14.4 ppm (C1), 22.7-24.8 ppm (C5), 31.9-35.7 ppm (C8), 29.1-29.5 ppm (C11), 29.1-29.5 ppm (C14), 29.2-32.3 ppm (C17), 29.0-29.3 ppm (C20), 29.0-29.3 ppm (C23), 25.7-29.6 ppm (C26), 25.4-25.6 ppm (C29), 29.5-34.7 (C32), and chemical shift of (C35) for hydrazide-hydrazone SB between 174.1-175.2 ppm (in DMSO-d_6), while theoretically at δ 10.9-15.1 ppm (C1), 25.1-27.7 ppm (C5), 35.5-37.3 ppm (C8), 34.1-36.0 ppm (C11), 34.2-35.8 ppm (C14), 33.9-36.4 ppm (C17), 33.9-35.7 ppm (C20), 33.1-35.8 ppm (C23), 33.3-35.7 ppm (C26), 25.6-32.4 ppm (C29), 34.8-39.6 ppm (C32), and 180.0-209.2 ppm (C35) (in DMSO) for compounds **2**, and **3a-c**. The ^{13}C NMR chemical shift for (C35) of compound **5** δ 164.8 ppm, and (C38) at 178.6 ppm (in $CDCl_3$) as experimentally, and theoretically at δ 188.3 ppm, 215.4 ppm (in DMSO) respectively. The carbon chemical value for (C40) (HC=N) imine experimentally between δ 169.0-169.6 ppm (in DMSO-d_6) and computed at δ 167.9-180.2 ppm (in DMSO). The carbon resonance signals of aromatic carbon are between δ 109.5-156.9 ppm (in DMSO-d_6) experimentally and theoretically between δ 112.3-162.8 ppm (in DMSO). The carbon resonance value for (HC=CH) group experimentally at δ 125.8 ppm (C17), and 148.1 ppm (C18) (in DMSO-d_6), while theoretically at 123.7 and 143.4 ppm (in DMSO) respectively. The calculated and observed ^{1}H and ^{13}C NMR chemical shift values provided conclusive evidence that the proposed structures of all of the compounds were correct.

3.3 FT-IR Analysis

When trying to determine whether or not organic compounds contain functional groups, infrared spectroscopy is an extremely helpful technique. Table 3 shows some of the characteristic IR assignments of compounds **2**, **3a-c**, and **5**. These results come from the previously mentioned study. Using a KBr pellet, we were able to experimentally record the vibrational frequencies of compounds **2**, **3a-c**, and **5** in the range of 4000-400 cm^{-1}. The DFT/B3LYP method, using a 6-311++G(d,p) basis in the gas phase, was used to calculate the theoretical IR frequency values for the optimized geometry. These values were used to determine the theoretical IR frequency values.

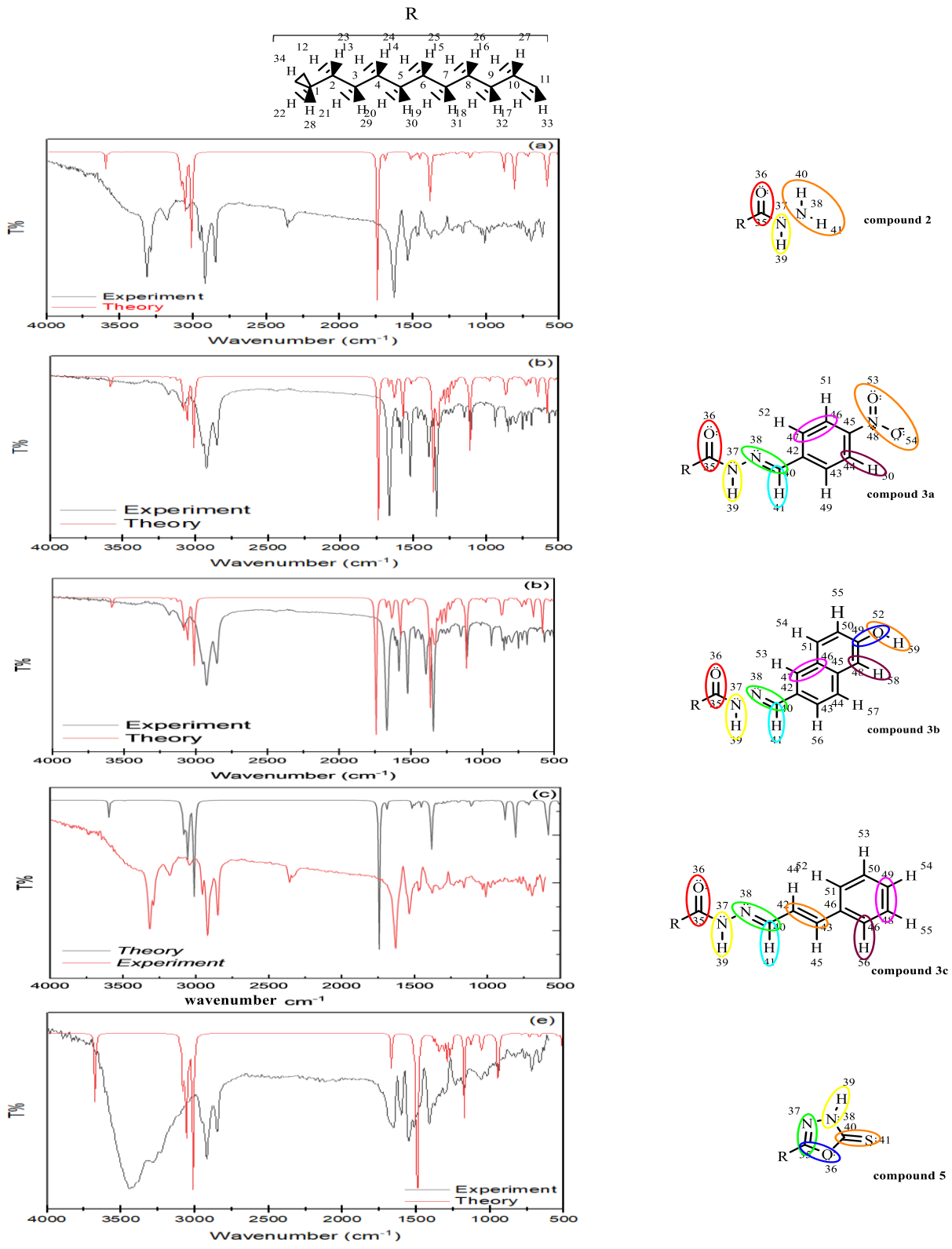

Fig. (1a-e): Theoretical and experimental vibrational analysis.

Table (3): Experimental and theoretical analysis of FT-IR spectroscopy for compounds(**2**, **3a-c**, and **5**)

Vibration assignment	Band position (cm^{-1})								
	Compound 2		Compound 3a		Compound 3b		Compound 3c		Compound 5
	Exp.	Theo.	Exp.	Theo.	Exp.	Theo.	Exp.	Theo.	Exp. Theo.
Alkanes									
C-H stretch	3043-2850	2991-3054	2924-2852	2992-3082	2920-2850	2990-3096	2920-2852	2992-3063	2920-2850 2991-3098
Imine									**C=N$_{heterocyclic}$**
=C-H stretch	–		3086	3075-3088	3051	3062	3049	3067	
C=N stretch	–		1598	1629-1668	1631	1635-1680	1544	1383-1688	1654 1668
Aromatic compounds									
=C-H stretch	–		2951	3174	2954	1155-1549	2954	3163-	–
C=C stretch	–		1581	1353-	1548-1467	1404-	3193		–
C-H bend			1638		1635		1467-1446	1330-	
							1688		
								1184-	
							1365		
Amine									–
-NH_2	3317-3290	3488-3596	–		–		–		
Alkene									
=C-H stretch	–		–		–		3199	3067	–
C=C stretch	–		–		–		1627	1608-	–
							1688		
Amide									**-N-H$_{heterocyclic}$**
N-H	3178	3596	3184	3583	3203	3577	3232	3578	3444
C=O	1631	1742	1666	1744	1664	1735	1666	1733	3675
									–
N-N	1010	1198-1207	1107	1105-	1114	1081	1114	1143	1068
			1135						1062
C-N	1381	1384	1257	1119	1182	1354	1195	655-1383	1415
									1494-1668
C-O					1153	1244			948
									946
N=O	–		1521	1366-1575	–		–		–
N-O	–		1342	1366-1575	–		–		–
C-C	979-617	897-1068	937-451	981-1066	947-478	842-1068	970-509	990-1067	1026-605
									897-1068
-OH	–		–		3234	3838	–		–
C=S	–		–		–		–		717
									541

3.4 UV-Vis spectroscopy

We have measured the UV-Vis electronic absorption spectra of compound (**2**, **3a-c**, and **5**) in the range of 250-650 nm in an organic solvent (DMSO and $CHCl_3$) at room temperature and a concentration $1x10^{-3}$M. In order to investigate the electronic absorption characteristics of the molecule in gas phase, the TD-DFT calculation approach based on the B3LYP/6-311++G(d, p) level for the optimized shape has been adopted. Figure 8 displayed the experimental and theoretical (TD-DFT) UV-Vis spectra, whereas Table 4 detailed the electronic transition values that corresponded to each spectrum.

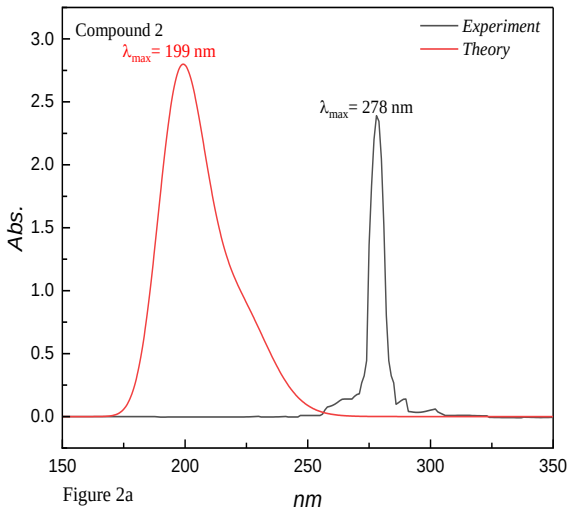

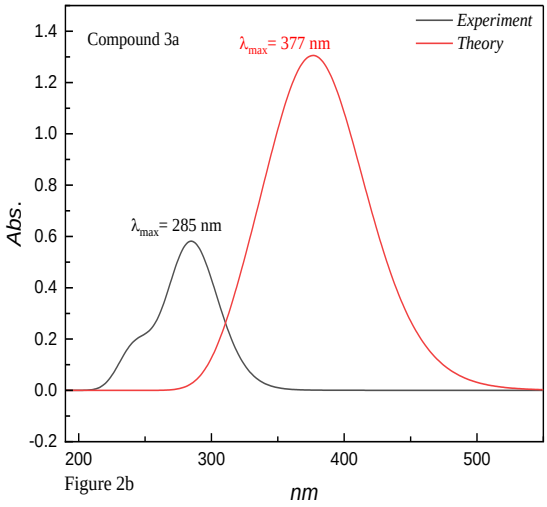

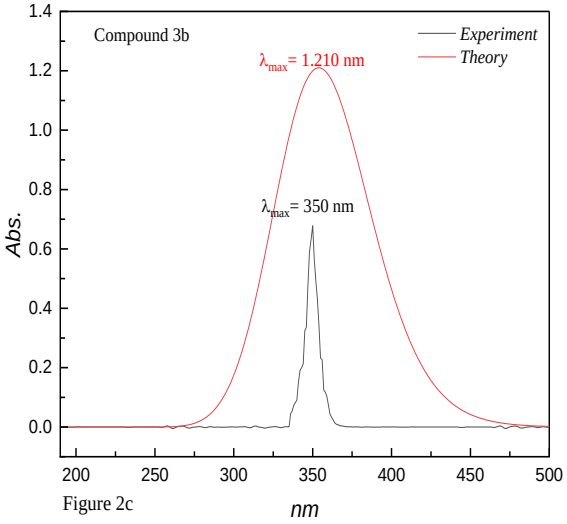

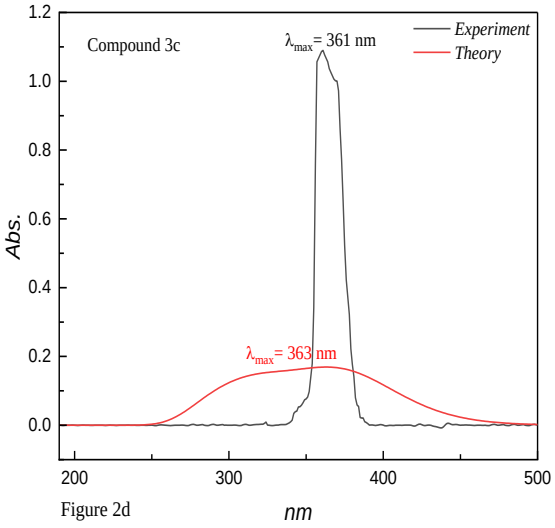

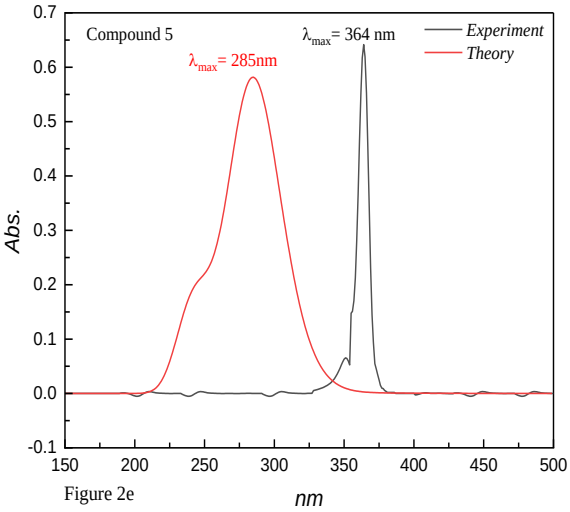

Fig. (2a-e): Experimental and theoretical UV-Vis spectra for compounds **2**, **3a-c**, and **5**.

Table (4): The experimental and theoretical UV-Vis spectroscopic parameters for compound (**2**, **3a-c**, and **5**)

Compounds	Experimental		Theoretical	
	λ_{max}(nm) (A=Absorption)	Solvent	λ_{max}(nm) (A=Absorption)	Solvent
2	**278**	**Chloroform**	**199**	**Gas phase**
3a	**285**	**Ethyl acetate**	**377**	**Gas phase**
3b	**350**	**Ethyl acetate**	**353**	**Gas phase**
3c	**361**	**Ethyl acetate**	**363**	**Gas phase**
5	**364**	**Chloroform**	**285**	**Gas phase**

Table 4 shows that the UV-Vis absorption bands for compounds (**2**, **3a-c**, and **5**) occurred at wavelengths between 278-364 nm when dissolved in organic solvents (ethyl acetate (EtOAc), and chloroform), despite having been theoretically calculated to be between 199-377 nm. The π-π^* transition of the azomethine and aromatic rings was found to be responsible for these maximal absorption bands.

3.5 Investigation of the HOMO and LUMO energies

The Highest Occupied Molecular Orbital (HOMO) is the ability of a molecule to donate an electron and the Lowest Unoccupied Molecular Orbital (LUMO) is the acquire an electron, they are terms from the theory of frontier molecular orbitals by using the Gaussian 09 distribution as shown in (Figure 3a-e) (Fukui, 1981; Özdemir Tari, Gümüş and Aɬar, 2015). Understanding the fundamental parameters that affect the electrical transport properties in the orbitals of a molecule is helpful for assessing the energy distribution and energetic behavior of a molecule. The capability of a molecule to give up or accept an electron is represented by ΔE_{Gap}.

In this study, various physical calculation parameters of compounds, such as global hardness (η), global softness (S), chemical potentials (IP), total energy, dipole moment (d.p.), global electrophilicity (ω), and absolute electronegativity (χ) were shown in Table 5 according to the following equations and optimized via DFT Method /B3LYP with 6-311++G(d,p)(Fahim *et al.*, 2021).

Ionization energy (I): $I = -E_{HOMO}$ …….. 1

Electronic affinity (A): $A = -E_{LUMO}$ …… 2

Energy Gap (ΔE_{Gap}): $\Delta E_{Gap} = E_{LUMO} - E_{HOMO}$ ……. 3

Global Hardness (η): $\eta = \frac{E_{LUMO} - E_{HOMO}}{2}$ ...…….. 4

Absolute Electronegativity (χ): $\chi = \frac{I+A}{2}$ …… 5

Chemical Softness (σ): $\sigma = \frac{1}{\eta}$ ……. 6

Table (5): Prepared hydrazide-hydrazone SB and oxadiazole electronic parameters (in a.u., 1 a.u. =27.211 ev, except dipole moment which is in the units of Debye) calculated using DFT/B3LYP theory.

compound	E_{HOMO}(ev)	E_{LUMO}(ev)	E_{Gap}(ev)	I	A	η	χ	σ	ω	Total energy	Dipole moment
2	-6.954398	-0.02393	6.30323	6.954398	0.651167	3.151616	3.802783	0.317298	2.294245	-657.8614	3.9294
3a	-6.976983	-0.12208	3.65502	6.97698	3.321959	1.827513	5.149471	0.547192	7.254958	-1131.631	2.4974
3b	-6.187310	-0.08435	3.892036	6.18973	2.295275	1.946018	4.241293	0.51387	5.042846	-1155.994	6.5109
3c	-6.221869	-0.0909	3.74836	6.221869	2.473509	1.87418	4.347689	0.533567	5.042846	-1004.490	5.1909
5	-6.355749	-0.03357	5.442265	6.55749	0.913484	2.721132	3.634617	0.367494	2.427379	-1092.982	4.4277

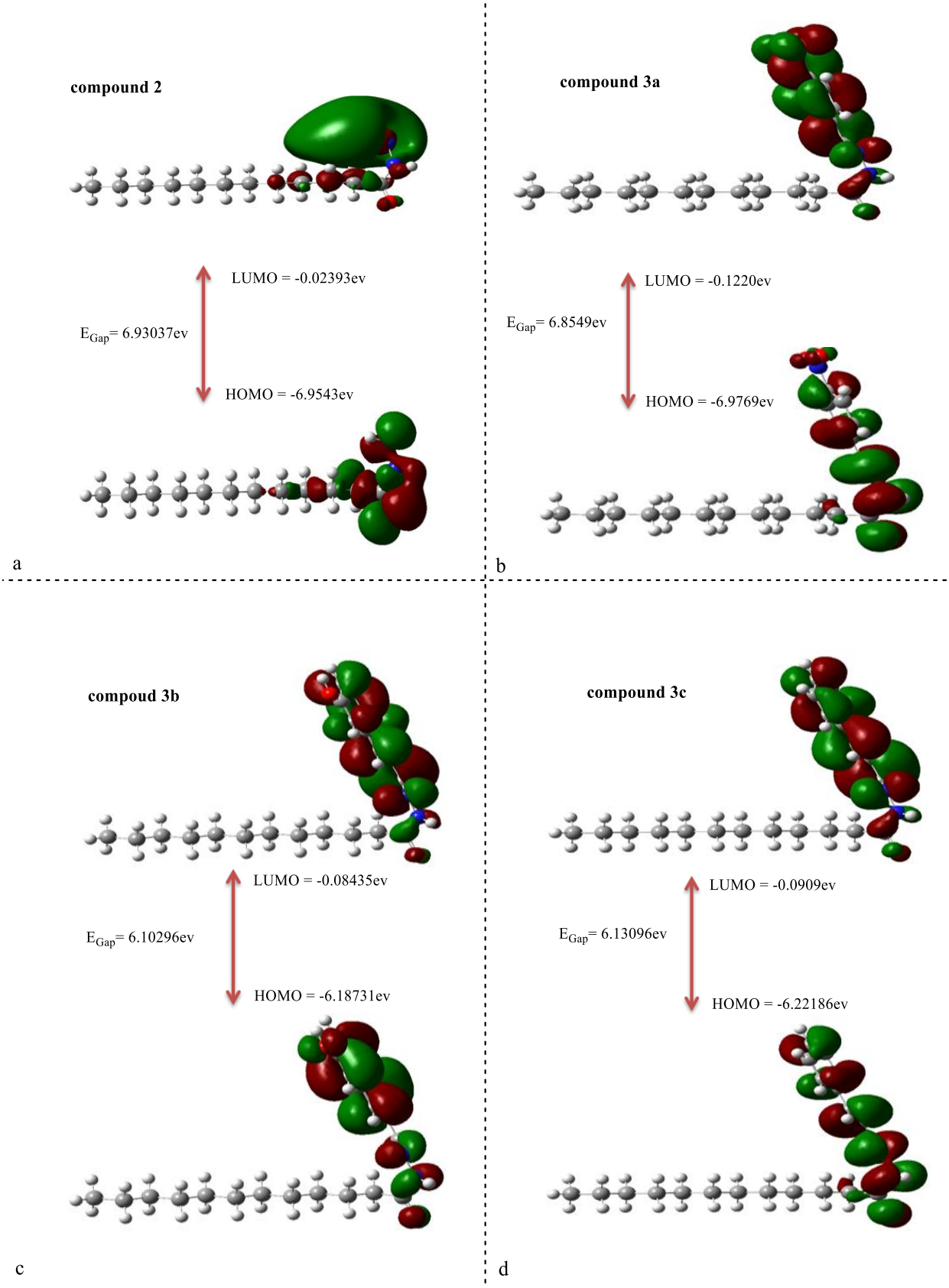
compound 2
LUMO = -0.02393ev
E_{Gap}= 6.93037ev
HOMO = -6.9543ev
a
compound 3a
LUMO = -0.1220ev
E_{Gap}= 6.8549ev
HOMO = -6.9769ev
b
compoud 3b
LUMO = -0.08435ev
E_{Gap}= 6.10296ev
HOMO = -6.18731ev
c
compound 3c
LUMO = -0.0909ev
E_{Gap}= 6.13096ev
HOMO = -6.22186ev
d

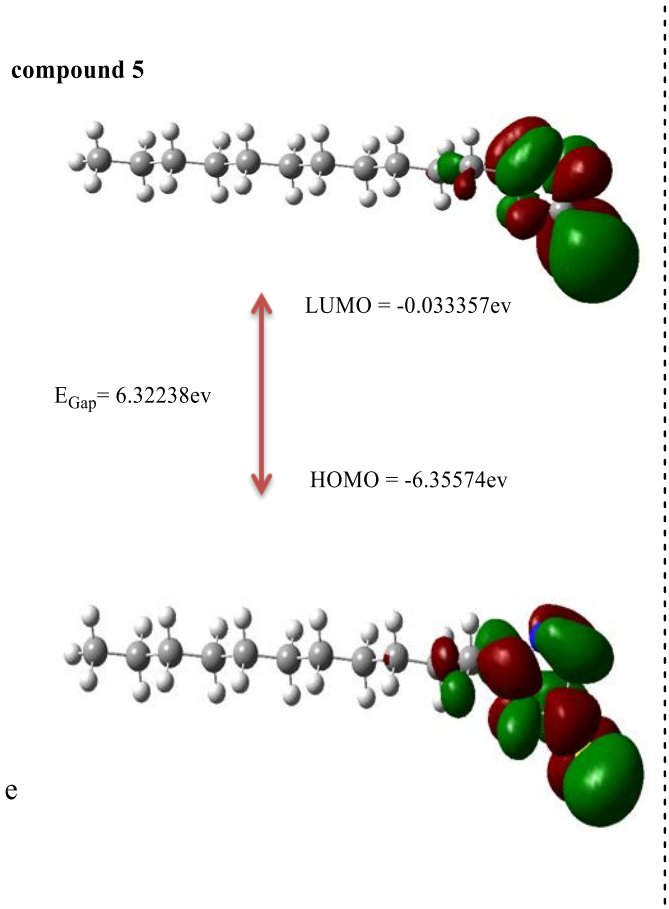

Fig. (3a-e): Using the B3LYP/6-311++G(d,p) method, we were able to obtain 3D plots of HOMO & LUMO for compounds **2**, **3a-c**, and **5**.

4. CONCLUSION

In this work, we synthesized a new Schiff bases derivative (compound **3a-c**) and 1,3,4-oxadiazole-2-thion that derived from Lauric acid and characterized it experimentally via ^{1}H & ^{13}C NMR, FT-IR, and UV-Vis spectroscopy. Gaussian 09 was used to improve the compound **2**, **3a-c**, and **5**'s geometry, IR vibration frequencies, ^{1}H and ^{13}C NMR chemical shifts, and HOMO LUMO energies at the DFT/B3LYP level of the theory with the 6-311++G(d, p) basis set. Experiment data were compared with the theoretical results for ^{1}H and ^{13}C NMR, FT-IR, and UV-Vis spectroscopy. The theoretical results for compounds (**2**, **3a-c**, and **5**) were modified so that they would be consistent with the experimental data. This compound's proposed structure is backed by both theory and experiment.

REFERENCES

(http://www.cambridgesoft.com/ (2015) 'ChemDrow 15'.

Abdulghani, A.J. and Abbas, N.M. (2011) 'Synthesis Characterization and Biological Activity Study of New Schiff and Mannich Bases and Some Metal Complexes Derived from Isatin and Dithiooxamide', 2011. Available at: https://doi.org/10.1155/2011/706262.

Aggoun, D. *et al.* (2021) 'Synthesis , characterization and DFT investigation of new metal complexes of Ni (II), Mn (II) and VO (IV) containing N , O-donor Schiff base ligand', *Journal of Molecular Structure*, 1231, p. 129923. Available at: https://doi.org/10.1016/j.molstruc.2021.129923.

Agregán, R. *et al.* (2022) 'Fatty acids', *Food Lipids: Sources, Health Implications, and Future Trends*, pp. 257–286. Available at: https://doi.org/10.1016/B978-0-12-823371-9.00015-0.

Aidi, M. *et al.* (2018) 'Pharmaceutical sciences research center , Kermanshah University of Medical Sciences , School of Chemistry , University of Melbourne , Victoria 3010 ,

Australia', *Inorganica Chimica Acta* [Preprint], (Ii). Available at: https://doi.org/10.1016/j.ica.2018.12.046.

Belaidi, O., Bouchaour, T. and Maschke, U. (2014) 'The molecular conformation of butyl acrylate - A vibrational spectroscopy and computational study', *Vibrational Spectroscopy*, 73, pp. 56–66. Available at: https://doi.org/10.1016/j.vibspec.2014.04.004.

Bendre, R.S., Tadavi, S.K. and Patil, M.M. (2017) 'Synthesis , crystal structures and biological activities of transition metal complexes of a salen - type ligand', *Transition Metal Chemistry* [Preprint]. Available at: https://doi.org/10.1007/s11243-017-0196-y.

Brahmkhatri, V. and Patel, A. (2012) 'Esterification of lauric acid with butanol-1 over H 3PW 12O 40 supported on MCM-41', *Fuel*, 102, pp. 72–77. Available at: https://doi.org/10.1016/j.fuel.2012.05.053.

Carpenter, C.A., Kenar, J.A. and Price, N.P.J. (2010) 'Preparation of saturated and unsaturated fatty acid hydrazides and long chain C-glycoside ketohydrazones', *Green Chemistry*, 12(11), pp. 2012–2018. Available at: https://doi.org/10.1039/c0gc00372g.

Elmacı, G. *et al.* (2019) 'SC', *Journal of Molecular Structure* [Preprint]. Available at: https://doi.org/10.1016/j.molstruc.2019.01.104.

Fahim, A.M. *et al.* (2021) 'Synthesis of novel β-lactams: Antioxidant activity, acetylcholinesterase inhibition and computational studies', *Journal of Molecular Structure*, 1233. Available at: https://doi.org/10.1016/j.molstruc.2021.130092.

Faraj, F.L. *et al.* (2019) 'Synthesis of New Indole Schiff Bases and Evaluation of Their Biological Activity on Lymphatic Cell in Metaphase in Human Blood', *Biochemical and Cellular Archives*, 19(2), pp. 4517–4524. Available at: https://doi.org/10.35124/bca.2019.19.2.4517.

Fukui, K. (1981) 'Fukui-Lecture.Pdf'.

Gökce, H. *et al.* (2017) 'Structural, spectroscopic, electronic, nonlinear optical and thermodynamic properties of a synthesized Schiff base compound: A combined experimental and theoretical approach', *Journal of Molecular Structure*, 1136, pp. 288–302. Available at: https://doi.org/10.1016/j.molstruc.2017.01.089.

Hiremath, S.M. *et al.* (2018) 'Synthesis of 5-(5-methyl-benzofuran-3-ylmethyl)-3H- [1, 3, 4] oxadiazole-2-thione and investigation of its spectroscopic, reactivity, optoelectronic and drug likeness properties by combined computational and experimental approach', *Spectrochimica Acta - Part A: Molecular and Biomolecular Spectroscopy*, 205, pp. 95–110. Available at: https://doi.org/10.1016/j.saa.2018.07.003.

January, R. (2013) 'Dinucleating Schiff base ligand in Zn / 4f coordination chemistry : Synthetic challenges and catalytic activity evaluation', 2(3), pp. 1–3. Available at: https://doi.org/10.1039/x0xx00000x.

Kajal, A. *et al.* (2013) 'Schiff Bases : A Versatile Pharmacophore', 2013(Mic).

Kargar, H. *et al.* (2021) 'Ultrasound-based synthesis , SC-XRD , NMR , DFT , HSA of new Schiff bases derived from 2-aminopyridine : Experimental and theoretical studies', *Journal of Molecular Structure*, 1233, p. 130105. Available at: https://doi.org/10.1016/j.molstruc.2021.130105.

Liu, X. *et al.* (2018) 'Multidentate unsymmetrically-substituted Schiff bases and their metal complexes : Synthesis , functional materials properties , and applications to catalysis', *Coordination Chemistry Reviews*, 357, pp. 144–172. Available at: https://doi.org/10.1016/j.ccr.2017.11.030.

M. J. Frisch, G. W. Trucks, H. B. Schlegel, G.E.S. *et al.* (2015) 'Gaussian 09, Revision D.01'.

Maniak, H. *et al.* (2020) 'Synthesis and structure-activity relationship studies of hydrazide-hydrazones as inhibitors of laccase from trametes versicolor', *Molecules*, 25(5). Available at: https://doi.org/10.3390/molecules25051255.

Nabhan, K.J. *et al.* (2022) 'New tetra-dentate schiff base ligand N2O2 and its complexes with some of metal ions: preparation, identification, and studying their enzymatic and biological activities', *Baghdad Science Journal*, 19(1), pp. 155–167. Available at: https://doi.org/10.21123/BSJ.2022.19.1.0155.

Orr, S.A., Andrews, P.C. and Blair, V.L. (2021) 'Main Group Metal-Mediated Transformations of Imines', *Chemistry - A European Journal*, 27(8), pp. 2569–2588. Available at: https://doi.org/10.1002/chem.202003108.

Özdemir Tari, G., Gümüş, S. and Aıar, E. (2015) 'Crystal structure, spectroscopic studies and quantum mechanical calculations of 2-[((3-iodo-4-methyl)phenylimino)methyl]-5-nitrothiophene', *Spectrochimica Acta - Part A: Molecular and Biomolecular Spectroscopy*, 141, pp. 119–127. Available at: https://doi.org/10.1016/j.saa.2015.01.050.

Parveen, S. (2020) 'Recent advances in anticancer ruthenium Schiff base complexes', *Applied Organometallic Chemistry*, 34(8), pp. 1–23. Available at: https://doi.org/10.1002/aoc.5687.

Qin, J.C. and Yang, Z.Y. (2016) 'Fluorescent chemosensor for detection of Zn2+ and Cu2+

and its application in molecular logic gate', *Journal of Photochemistry and Photobiology A: Chemistry*, 324, pp. 152–158. Available at: https://doi.org/10.1016/j.jphotochem.2016.03.029.

Qin, W. *et al.* (2013) 'Schiff Bases: A Short Survey on an Evergreen Chemistry Tool', (April 1834), pp. 12264–12289. Available at: https://doi.org/10.3390/molecules181012264.

Raczuk, E. *et al.* (2022) 'Different Schiff Bases—Structure, Importance and Classification'.

Rosaleen J. Anderson, D.J.B. and P.W.G. (2010) *Organic Spectroscopic Analysis*, *Antimicrobial Agents and Chemotherapy*. Available at: http://www.ncbi.nlm.nih.gov/pubmed/25246403%0Ahttp://www.pubmedcentral.nih.gov/articlerender.fcgi?artid=PMC4249520%0Ahttp://aac.asm.org/lookup/doi/10.1128/AAC.03728-14%0Ahttp://arxiv.org/abs/1011.1669%0Ahttp://dx.doi.org/10.1088/1751-8113/44/8/085201.

Sherif, O.E. and Abdel-kader, N.S. (2015) 'DFT calculations , spectroscopic studies , thermal analysis and biological activity of supra molecular Schiff base complexes', *ARABIAN JOURNAL OF CHEMISTRY* [Preprint]. Available at: https://doi.org/10.1016/j.arabjc.2015.07.008.

Singh, G. *et al.* (2021) 'A quick microwave preparation of isatin hydrazone schiff base conjugated organosilicon compounds : Exploration of their antibacterial , antifungal , and antioxidative potentials', *Journal of Organometallic Chemistry*, 953, p. 122051. Available at: https://doi.org/10.1016/j.jorganchem.2021.122051.

Singh, N., Ranjana, R. and Kumari, M. (2016) 'A Review on Biological Activities of Hydrazone Derivatives', 8(3), pp. 162–166.

Singh, R.K. *et al.* (2017) 'Synthesis, molecular structure, spectral analysis and cytotoxic activity of two new aroylhydrazones', *Journal of Molecular Structure*, 1135, pp. 82–97. Available at: https://doi.org/10.1016/j.molstruc.2017.01.059.

Sıcak, Y. *et al.* (2019) 'Novel fluorine-containing chiral hydrazide-hydrazones: Design, synthesis, structural elucidation, antioxidant and anticholinesterase activity, and in silico studies', *Chirality*, 31(8), pp. 603–615. Available at: https://doi.org/10.1002/chir.23102.

Srivastava, K.P., Yadav, U.S. and Singh, P. (2021) 'EVALUATION OF ANTIMICROBIAL ACTIVITIES OF MICROWAVE-IRRADIATION SYNTHESIZED TETRADENTATE (N 2 O 2 DONOR) SCHIFF BASE AND ITS Cu (II) COMPLEXES', 14(4), pp. 2604–2612.

Su, X. *et al.* (2013) 'Manipulating Liquid-Crystal Properties Using a pH Activated Hydrazone Switch', *Angewandte Chemie*, 125(41), pp. 10934–10939. Available at: https://doi.org/10.1002/ange.201305514.

Tidwell, T.T. (2008) 'Hugo (Ugo) Schiff , Schiff Bases , and a Century of b -Lactam Synthesis **', pp. 1016–1020. Available at: https://doi.org/10.1002/anie.200702965.

Turan, B. *et al.* (2016) 'The synthesis of some β -lactams and investigation of their metal-chelating activity , carbonic anhydrase and acetylcholinesterase inhibition profiles', 6366. Available at: https://doi.org/10.3109/14756366.2016.1170014.

Wu, B.X. *et al.* (2021) 'Synthesis, photochemical isomerization and photophysical properties of hydrazide-hydrazone derivatives', *New Journal of Chemistry*, 45(3), pp. 1651–1657. Available at: https://doi.org/10.1039/d0nj05172a.

Wu, J. *et al.* (2021) 'Synthesis and Cytotoxic Activity of Novel Betulin Derivatives Containing Hydrazide-Hydrazone Moieties', *Natural Product Communications*, 16(10), pp. 4–10. Available at: https://doi.org/10.1177/1934578X211055345.

Yang, Z.B., Li, P. and He, Y.J. (2020) 'Novel pyrethrin derivatives containing hydrazone and 1,3,4-oxadiazole thioether moieties: Design, synthesis, and insecticidal activity', *Phosphorus, Sulfur and Silicon and the Related Elements*, 195(8), pp. 614–619. Available at: https://doi.org/10.1080/10426507.2019.1700416.

Zhang, Y., Xu, X. and Goddard, W.A. (2009) 'Doubly hybrid density functional for accurate descriptions of nonbond interactions, thermochemistry, and thermochemical kinetics', *Proceedings of the National Academy of Sciences of the United States of America*, 106(13), pp. 4963–4968. Available at: https://doi.org/10.1073/pnas.0901093106.

Zhou, B. *et al.* (2009) 'Study on THz spectrum of artemeter', *Journal of Molecular Structure*, 919(1–3), pp. 325–327. Available at: https://doi.org/10.1016/j.molstruc.2008.09.025.